THE JOURNAL OF BIOLOGICAL CHEMISTRY
Vol. 278, No. 27, Issue of July 4, pp. 24688–24696, 2003

Printed in U.S.A.

Isoform Heterogeneity of the Human Gephyrin Gene (*GPHN*), Binding Domains to the Glycine Receptor, and Mutation Analysis in Hyperekplexia*

Received for publication, January 31, 2003, and in revised form, April 5, 2003
Published, JBC Papers in Press, April 8, 2003, DOI 10.1074/jbc.M301070200

Mark I. Rees‡§, Kirsten Harvey¶, Hamish Ward‡, Julia H. White‖, Luc Evans, Ian C. Duguid¶‡‡, Cynthia C.-H. Hsu‡, Sharon L. Coleman§§, Jan Miller‡, Kristin Baer‡, Henry J. Waldvogel¶¶, Francis Gibbon‖‖, Trevor G. Smart¶‡‡, Michael J. Owen‡, Robert J. Harvey¶, and Russell G. Snell‡**

*From the Departments of ‡Molecular Medicine and ¶¶Anatomy, Faculty of Medical and Health Sciences, University of Auckland, Private bag 92019, Auckland, New Zealand, the ¶Department of Pharmacology, School of Pharmacy, 29-39 Brunswick Square, London WC1N 1AX, United Kingdom, ‖Pathway Discovery, Genomics and Proteomic Sciences, GlaxoSmithKline Medicines Research Centre, Gunnels Wood Road, Stevenage SG1 2NY, United Kingdom, **University of Birmingham Medical School, Birmingham B15 2TT, United Kingdom, the §§Department of Psychological Medicine, University of Wales College of Medicine, Heath Park, Cardiff CF14 4XN, United Kingdom, the ‖‖Department of Paediatric Neurology, University Hospital of Wales, Heath Park, Cardiff CF14 4XN, United Kingdom*

Gephyrin (GPHN) is an organizational protein that clusters and localizes the inhibitory glycine (GlyR) and $GABA_A$ receptors to the microtubular matrix of the neuronal postsynaptic membrane. Mice deficient in gephyrin develop a hereditary molybdenum cofactor deficiency and a neurological phenotype that mimics startle disease (hyperekplexia). This neuromotor disorder is associated with mutations in the GlyR α_1 and β subunit genes (*GLRA1* and *GLRB*). Further genetic heterogeneity is suspected, and we hypothesized that patients lacking mutations in *GLRA1* and *GLRB* might have mutations in the gephyrin gene (*GPHN*). In addition, we adopted a yeast two-hybrid screen, using the GlyR β subunit intracellular loop as bait, in an attempt to identify further GlyR-interacting proteins implicated in hyperekplexia. Gephyrin cDNAs were isolated, and subsequent RT-PCR analysis from human tissues demonstrated the presence of five alternatively spliced *GPHN* exons concentrated in the central linker region of the gene. This region generated 11 distinct *GPHN* transcript isoforms, with 10 being specific to neuronal tissue. Mutation analysis of *GPHN* exons in hyperekplexia patients revealed a missense mutation (A28T) in one patient causing an amino acid substitution (N10Y). Functional testing demonstrated that $GPHN^{N10Y}$ does not disrupt GlyR-gephyrin interactions or collybistin-induced cell-surface clustering. We provide evidence that GlyR-gephyrin binding is dependent on the presence of an intact C-terminal MoeA homology domain. Therefore, the N10Y mutation and alternative splicing of GPHN transcripts do not affect interactions with GlyRs but may affect other interactions with the cytoskeleton or gephyrin accessory proteins.

Neuronal postsynaptic membranes contain a wide variety of ion channels and receptor proteins that contribute to the balance of excitatory and inhibitory neurotransmission in the human central nervous system. Mature postnatal neuroinhibition is mediated by postsynaptic glycinergic and $GABA_A$[1] receptor systems that are structurally related to the nicotinic receptors with a typical pentameric structure constructed from heterogeneous subunit constituents containing four transmembrane (TM) domains and a large intracellular loop between TM3 and TM4 (1, 2). These subunits combine to form fast response, ligand-gated chloride channels that modify excitatory neurotransmission in the human brainstem and spinal cord (3–5). Inhibitory glycine receptors (GlyRs) are composed of three ligand-binding α_1 subunits (GlyR α_1) and two structural β subunits (GlyR β) that are anchored and clustered on the postsynaptic membrane of inhibitory neurons by the interaction of a motif within the TM3-TM4 loop of the GlyRβ subunit with anchoring protein, gephyrin (6–8). In contrast to GlyRs, there is a lack of evidence for a direct physical interaction between gephyrin and $GABA_A$ receptor subunit(s) (7, 9), although immunohistochemical studies have detected co-localization of gephyrin with major subtypes of $GABA_A$ receptors at GABAergic postsynaptic sites in murine and rat brain (10–14).

Gephyrin (GPHN) belongs to a group of cytoskeletal elements that are critical for receptor-associated synaptic localization and organization. First identified as a 93-kDa protein by co-purification with GlyRs from rat spinal cord, GPHN demonstrated high affinity binding to tubulin (15–17). It is suggested that gephyrin forms a postsynaptic organizational lattice structure that dynamically immobilizes and clusters inhibitory receptors onto the cytoskeletal infrastructure (14, 18). In support of this, GPHN-dependent postsynaptic clustering of GlyRs was demonstrated by cellular antisense experi-

* This work was supported by grants from the Wellcome Trust, Auckland Medical Research Foundation, and the Freemasons of New Zealand (New Zealand) (to R. G. S. and M. I. R.) and the Medical Research Council (United Kingdom) (to R. J. H. and T. G. S.). The costs of publication of this article were defrayed in part by the payment of page charges. This article must therefore be hereby marked "*advertisement*" in accordance with 18 U.S.C. Section 1734 solely to indicate this fact.

§ To whom correspondence should be addressed. Tel.: 64-9-373-7599 (ext. 4486); Fax: 64-9-373-7492; E-mail: m.rees@auckland.ac.nz.

‡‡ Present address: Dept. of Pharmacology, University College London, Gower Street, London WC1E 6BT, United Kingdom.

[1] The abbreviations used are: $GABA_A$, γ-aminobutyric acid type A; GPHN, gephyrin; GlyR, glycine receptor; *GLRA1*, α_1-subunit gene of GlyRs; *GLRB*, β-subunit gene of GlyRs; GlyR α_1, α_1-subunit polypeptide of GlyRs; GlyR β, β-subunit polypeptide of GlyRs; TM, transmembrane domain; RT, reverse transcriptase; YTH, yeast two-hybrid; SNP, single nucleotide polymorphism; BAC, bacterial artificial chromosome; SSCP, single-stranded conformation polymorphism; DDF, dideoxy fingerprinting; dHPLC, denaturing high performance liquid chromatography; contig, group of overlapping clones; TRITC, tetramethylrhodamine isothiocyanate; EGFP, enhanced green fluorescent protein.

ments and from studies of a *gphn* knock-out mouse model (12, 19, 20). Heterogeneous roles for gephyrin have been implicated by protein-protein interactions with a range of determinants such as RAFT1, tubulin, profilin, collybistin, and the dynein light chains 1 and 2 (17, 21–24).

The preliminary structure of the gephyrin gene (*GPHN*) has been described in mice and humans (25–27), although there is a degree of ambiguity in the number of exons due to the presence of multiple transcript isoforms, and it is uncertain that all exons have been located and identified. Indeed, *GPHN* expression is not restricted to rat brain and spinal cord but is also found in liver, kidney, lung, and retina (28–30). Gephyrin knock-out mice and reconstitutive cell culture assays have demonstrated that gephyrin expression in nonneuronal tissue is a requirement for the biosynthesis of molybdenum cofactor (20, 31). Striking homologies are observed between the primary structure of GPHN and proteins involved in bacterial, plant, and invertebrate molybdenum cofactor biosynthesis. Gephyrin, therefore, has a synaptic function as a postsynaptic anchoring and clustering protein in neurons while facilitating a highly conserved metabolic purpose in nonneuronal tissues (32). The genetic and structural basis of the functional dichotomy is not established; however, in rats, a putative explanation may lie in the generation of distinct transcript isoforms of gephyrin constructed from alternative splicing of eight exonic "cassettes" within four regions of GPHN (25, 28, 33). Apart from conferring neuronal and nonneuronal characteristics to the mature polypeptide products, the purpose of the transcript heterogeneity pattern is unclear, and the number of isoform combinations in human tissue remains unestablished.

In addition to major disruption of molybdenum cofactor biosynthesis, gephyrin-deficient mice display a neuromotor phenotype, which resembles human hereditary hyperekplexia. This neurological condition (Mendelian Inheritance of Man: 149400 and 138491) can be caused by dominant and recessive mutations in the *GLRA1* and *GLRB* receptor genes and is characterized by an abnormal, persistent startle response to unexpected stimuli, neonatal hypertonia, and a chronic accumulation of injuries caused by unprotected, startle-induced falls (34–40). Furthermore, autoimmunity to GPHN was detected in a patient with Stiff-Man syndrome, a disorder that has a degree of phenotypic overlap with hyperekplexia (41). Collectively, this indicates that GPHN is a candidate gene for neurological and metabolic disorders, and support for the latter has recently emerged with a description of a GPHN reading frame mutation in a family with hereditary molybdenum cofactor deficiency (42).

In response to the candidacy of gephyrin for hyperekplexia, we pursued the definitive genomic structure of gephyrin by a combination of *in silico* BAC contig construction and multitissue RT-PCR methods. Using a yeast two-hybrid (YTH) screen, with the GlyR β subunit intracellular loop as bait, we attempted to identify further GlyR-interacting proteins that might be implicated in hyperekplexia. The results of this screen, together with the extensive search for all human *GPHN* transcripts in both neuronal and nonneuronal tissues, suggest the presence of one new *GPHN* exon and at least 11 neurological transcript isoform combinations that redefine the genomic organization of *GPHN*. Having established the number of exons in the *GPHN* gene, we completed a systematic exon by exon mutation analysis of *GPHN* in a cohort of hyperekplexia patients devoid of *GLRA1* and *GLRB* mutations. One novel mutation (N10Y) and several SNPs are reported; however, the functional effect of the mutation remains elusive despite assays for receptor targeting and clustering. We also present evidence that GlyR-gephyrin binding is dependent on the presence of an intact C-terminal MoeA homology domain and that the heterogeneous GPHN linker region is not the physical determinant for gephyrin-GlyR binding.

MATERIALS AND METHODS

RT-PCR Analysis of GPNH Alternative Splicing—A *GPHN* gene-specific primer (Table I) was used in a first-strand cDNA synthesis reaction (SuperScript II; Invitrogen) from total RNA derived from adult brain, fetal brain, cerebellum, and human spinal cord (Clontech). In addition to neurological tissue, cDNA was synthesized from a selection of nonneurological tissues including heart, liver, lung, kidney, trachea, fetal liver, pancreas, and placenta (Clontech). In the first instance, exonic primers were designed in constitutional regions surrounding the candidate regions of alternative splicing, namely regions C1/2, C3, C4/5, and C6/7 (Table I). To validate the initial RT-PCR methodology, downstream nested primers within the *GPHN* spliced exons were used in conjunction with primers from upstream invariant portions of the *GPHN* message (Table I). In the presence of multiple PCR products, DNA fragments were cloned into pGEM-Easy vectors (Stratagene), and the transformants were PCR-screened and assessed for size differences by molecular screening agarose (Roche Applied Sciences) and 10% nondenaturing polyacrylamide gels (Sigma). Minipreparations of clones were digested with *Eco*RI, and inserts were sequenced using ABI 3100 technology.

YTH Screening—To identify GlyR β subunit interactors in human brain, we cloned the large intracellular loop of the human GlyR β subunit into the plasmid vector pYTH9 (43, 44). In this manner, the large TM3-TM4 intracellular loop (known to harbor a gephyrin binding motif) (8) was fused to the GAL4 DNA binding domain. pYTH9 is advantageous for YTH screening, since the bait plasmid can be stably integrated into the yeast genome at the *trp-1* locus. An adult human brain cDNA library in pACT2 (HL4004AH; Clontech) was be screened by transformation of library DNA into the pYTH9-GlyR β yeast strain. Transformed yeast were plated on selective dropout media lacking leucine, tryptophan, and histidine, supplemented with 10 mM 3-amino-1,2,4-triazole, a competitive inhibitor of the *HIS3* gene product. Transformation plates were incubated at 30 °C for 12 days to allow histidine prototropic colonies to emerge. Surviving colonies were restreaked onto selective agar, lifted onto Whatman 54 paper, and screened for protein-protein interactions using a standard freeze-thaw fracture assay for the *lacZ* reporter gene (44). Library plasmid DNAs were recovered from β-galactosidase-positive colonies using the Yeastmaker plasmid isolation kit (Clontech), transformed into *Escherichia coli* XL1-blue (Stratagene), miniprepped, and sequenced. True interactions were checked by retransformation of library plasmids into yeast containing pYTH16 (an episomal version of pYTH9) and pYTH16-GlyR β. Library plasmids that were capable of autoactivation (*i.e.* activated *lac*Z with pYTH16 alone) were excluded from further analysis.

Constructs, Human Embryonic Kidney (HEK) Cell Transfection, and Confocal Microscopy—For the pDSRed-GlyR β construct, the large intracellular loop of the human GlyR β subunit was amplified using the primers BDSRed1 (5′-GCTGAATTCGCCACCATGGCAGTTGTCCAGGTGATGCT-3′) and BDSRed2 (5′-AACGGATCCCTTGCATAAAGATCAATTCGC-3′) and cloned into the *Eco*RI and *Bam*HI sites of pDSRed-N1 (Clontech). For the pEGFP-gephyrin construct, the entire coding region of the rat gephyrin P1 isoform (28) was amplified using the primers G1 (5′-CGCTGATCAACATGGCGACCGAGGGA-3′) and G14 (5′-TGGCTCGAGTCATAGCCGTCCGATGA-3′), cut with *Bcl*I and *Xho*I, and cloned into the *Bgl*II and *Sal*I sites of pEGFPC2 (Clontech). The N10Y mutation was introduced into pEGFP-gephyrin by site-directed mutagenesis, using 27-mer oligonucleotides and the QuikChange kit (Stratagene). Collybistin cDNAs were amplified from postnatal (P0) rat brain first-strand cDNA using the primers CB1 (5′-GTGGGATCCATGCAGTGGATTAGAGGCGGA-3′) and CB3 (5′-TTAGAATTCTCTGCCTTCCTATAGGTATTA-3′ and cloned into the *Bam*HI and *Eco*RI and sites of the vector pRK5myc. The construct used in this study (pRK5mycCB2SH3−) encodes the collybistin II isoform (23). All amplifications were performed using *Pfu Turbo* proofreading DNA polymerase (Stratagene), and DNAs for transfection were made using the Plasmid Maxi Kit (Qiagen). All constructs were sequenced using the BigDye ready reaction mix (PerkinElmer Life Sciences) and an ABI 310 automated DNA sequencer (Applied Biosystems).

HEK cells (ATCC CRL1573) were grown in Dulbecco's modified Eagle's medium supplemented with 10% fetal calf serum, 2 mM glutamine, 100 units ml^{-1} penicillin G, and 100 mg ml^{-1} streptomycin at 37 °C in 95% air-5% CO_2 (45). Exponentially growing cells were electroporated (400 V, infinite resistance, 125 microfarads; Bio-Rad Gene Electro-

pulser II) with various combinations of three plasmid constructs: pDSRed-GlyR β, pEGFP-gephyrin^{N10Y}, or pRK5myc-collybistin II. After 24 h, cells were washed twice in phosphate-buffered saline and fixed for 5 min in 4% (w/v) phosphonoformic acid (PFA) in phosphate-buffered saline. Myc-tagged collybistin II was detected using an anti-9E10 monoclonal antibody (Sigma) and TRITC-conjugated secondary antibodies (Jackson ImmunoResearch) using standard protocols. Confocal microscopy was performed as previously described (46).

In Silico Determination of Human Gephyrin Gene Structure—Rat cDNA (28) and human expressed tag sites similar to rat gephyrin were submitted for BLAST searches (available on the World Wide Web at www.ncbi.nlm.nih.gov/BLAST/). Portions of rat cDNA fragments displayed 90–95% homology with dispersed regions of several chromosome 14 human genome BACs submitted to GenBank™. Exon/intron organization was established from the genomic BAC contig, and a putative promoter region was identified through sequence homologies. Details of the human *GPHN* gene have subsequently been described by David-Watine (27), and the BAC clones are accessible from GenBank™.

Hyperekplexia Patients—The majority of patients included in the mutation analysis of the *GPHN* gene (n = 31) are described elsewhere (37). In addition, a further seven unrelated hyperekplexia patients all exhibited to the diagnostic criteria of inclusion, which involves a history of neonatal hypertonia, a nose tap response, and an exaggerated startle response, leading to injurious fall down consequences with preservation of consciousness.

PCR Analysis of GPHN in Hyperekplexia—The *GPHN* promoter region, exons and flanking intronic sequences, and 5′- and 3′-untranslated regions were amplified from patient DNA. Primer sets were designed by Primer 3.0 criteria via the online facility (available on the World Wide Web at www-genome.wi.mit.edu/cgi-bin/primer/primer3.0). Each 25-μl reaction contained 60 ng of genomic DNA, 10 pmol of each primer, 1.5 mM $MgCl_2$, 50 mM KCl, 10 mM Tris-HCl (pH 8.3), 200 μM dNTPs (Amersham Biosciences), and 1 unit of *Taq* polymerase (Qiagen). Promoter regions were amplified with Expand Fidelity *Taq* (Roche Applied Science) accompanied by 10% (v/v) Me_2SO (Sigma) because of the high GC content of the region. The DNA was amplified in MJ Research or PerkinElmer Life Sciences thermocyclers.

SSCP—Samples for screening were prepared by denaturing 5 μl of *GPHN* PCR products with 7 μl of formamide dye at 94 °C for 5 min. Samples were cooled and applied to 10% nondenaturing gels (49:1; Sigma) and run at 75 V for 12–16 h at room temperature and 4 °C. All SSCP gels were silver-stained as previously described (47).

Bidirectional Dideoxy Fingerprinting (DDF) Analysis—DDF analysis was carried out using [α-^{33}P]ddNTP/dNTP mixtures and thermosequenase reactions (Amersham Biosciences). DDF patterns for *GPHN* assays were resolved on MDE nondenaturing gels (48, 49).

dHPLC—Analysis was carried out using the Transgenomics dHPLC 2100 WAVE^R DNA Fragment Analysis System and DNASep^R column (Transgenomic, Santa Clara, CA). The dHPLCMelt program was used to predict the optimal melting conditions for PCR fragments, which were analyzed on a WAVE DNA fragment analyzer at temperatures recommended by predicted helicity profiles across the DNA fragment. Variant dHPLC profiles suggestive of sequence heterogeneity were sequenced. The WAVE was run under partially denaturing conditions for mutation detection and SNP discovery. Wavemaker 4.0 software was used to control the rate of flow of buffers and column running. A volume of between 4 and 8 μl of patient and control PCRs were injected into the column depending on the DNA concentration of the PCR.

DNA Sequencing—GPHN SNPs were detected by radionucleotide [α-^{33}P] cycle sequencing. Sequencing was initiated using a denaturation stage at 94 °C for 5 min followed by 45 cycles of primer annealing temperatures at 55 °C for 30 s, primer extension at 72 °C for 1 min, and denaturation at 94 °C for 30 s. Denatured samples were applied to a 6% denaturing polyacrylamide gels (Sigma) and resolved at 85 watts for 1–2 h at room temperature. The sequence content of RT-PCR products and clones were determined by ABI 3100 equipment using BigDYE chemistry (PerkinElmer Life Sciences). Each amplimer was sequenced with sense and antisense primers using an ABI PRISM™ BigDye Terminator cycle sequencing kit and AmpliTaq DNA polymerase (PerkinElmer Life Sciences).

Population Studies—The population frequency of identified sequence variations (potentially pathogenic mutations and SNPs) were established in a variable number of unrelated controls of Caucasian descent and derived from blood donor clinics in New Zealand (Table II). In instances where a restriction site change was predicted by the polymorphism, the relevant restriction fragment length polymorphism assay was designed and resolved by agarose gel electrophoresis or polyacrylamide gel electrophoresis. For those SNPs devoid of restriction site changes, the SNP frequency in the normal population was determined by comparison of mutation profiles *versus* normal profiles using mutation screening techniques SSCP, DDF, or dHPLC (see Table II).

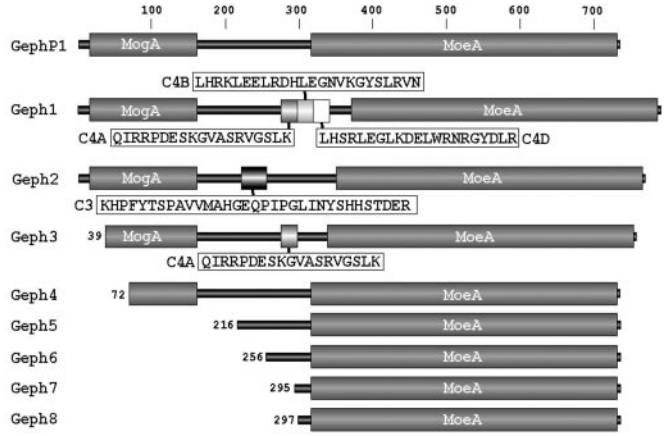

FIG. 1. **Gephyrin clones captured by yeast two-hybrid screen.** Shown is a schematic diagram displaying the domain structure of the human gephyrin P1 isoform (GephP1) indicating the positions of the MogA and MoeA homology domains (amino acids 16–169 and 323–736) and the intervening "linker" segment (amino acids 170–322). Below this are the structures of the human gephyrin cDNAs isolated in our GlyR β subunit YTH screen (Geph1–Geph8). Note that some cDNAs contained either C3 (Geph2) or single (Geph3) or multiple (Geph1) C4 cassettes. In addition, all cDNAs encode an intact MoeA homology domain, suggesting that this region is essential for mediating robust interactions with the GlyR β subunit.

RESULTS

GlyR β Subunit YTH Screen—In an attempt to identify further GlyR-interacting proteins that may be implicated in hyperekplexia, we carried out a YTH screen of an adult human brain cDNA library, using the GlyR β subunit TM3-TM4 intracellular loop as bait. The cDNA library had an original complexity of 3.5×10^6 independent cDNA clones, and 8×10^6 cDNAs were screened. Twelve positive clones were recovered, which specifically interacted with the GlyR β subunit bait. These represented eight independent cDNAs encoding variants of the human homologue of *GPHN* (Fig. 1). No other interacting proteins were found. Some of our gephyrin cDNAs (*e.g.* Geph1) were full-length, which allowed us to predict the entire coding sequence of the human gephyrin polypeptide. Structurally, the N- and C-terminal domains of gephyrin show high similarity to *E. coli* proteins (MogA and MoeA), a *Drosophila* protein (CINNAMON), and an *Arabidopsis thaliana* protein (CNX1), all of which are involved in the synthesis of a molybdenum-containing co-factor essential for molybdoenzyme activity. Analysis of the phylogenetic conservation within the human *GPHN* open reading frame reveals a 94% homology to rodent *gphn* sequence and a 91% homology to chicken sequence, assuming the exclusion of all alternatively transcribed exons. In comparison with rodents, this is translated into a 99.7% amino acid conservation (Fig. 2) within the constitutional 736-amino acid reading frame. Degeneracy is observed at two sites, I240L and A242R, amino acid changes that lie immediately 5′ adjacent to the C3 linker insertion site (30). The amino acid conservation between chicken and human GPHN is reduced to 98.7%, with all but one of the nine degenerate changes occurring at the MoeA domain, and a reversal of the rodent I240L and A242R changes is observed (Fig. 2).

Interestingly, several of the GlyR β-interacting GPHN clones (Geph5–8) were missing all of the N-terminal MogA homology domain (amino acids 16–169) as well as most of the "linker" segment of gephyrin (amino acids 170–322; Fig. 1). This suggests that an intact C-terminal MoeA domain is required for

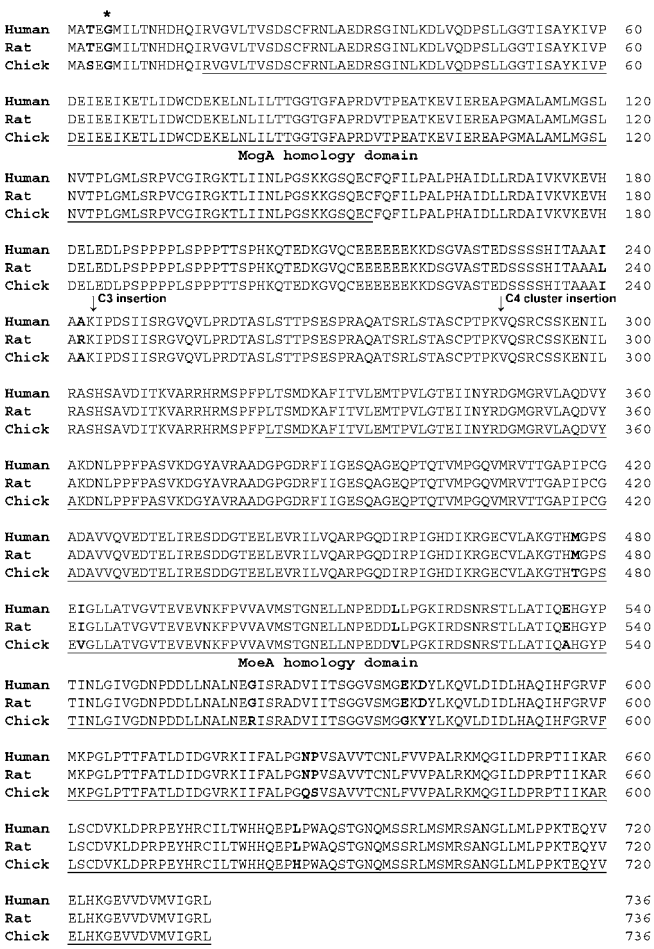

FIG. 2. **Phylogenetic alignment of GPHN.** Shown is amino acid alignment of human, rodent, and chicken GPHN, with *shaded regions* representing points of divergence from the human sequence. The *arrows* indicate the insertion points for the C3 and C4 cluster exons within the linker region of GPHN. The alignment does not include the C3/C4 cluster exons in the linker region, but there is 100% conservation with rat C3 and C4 exons, whereas no comparative data are available for chicken gephyrin. The MogA and MoeA regions are indicated by *underlined segments* of the alignment, and the position of a putative myristoylation site (*) is indicated (26).

strong interactions with the GlyRβ subunit and that the binding site on gephyrin for GlyRs does not reside in the MogA homology domain or the linker region.

Transcript Heterogeneity of Human GPHN—Several variants of gephyrin were found in our GlyR β subunit YTH screen. That gephyrin exists in multiple isoforms has been established for some time (25, 28, 33); the most common variants have insertions in the "linker" region, where exon C3 inserts the peptide NHPFYTSPAVFMANHGQPIPGLISYSHHATGSADKR between amino acids 243 and 244, and the C4 exon inserts the sequence ARLPSCSSTYSVSE between amino acids 288 and 289. More recently, Ramming *et al.* (25) described seven alternatively expressed murine exons including three consecutive C4 exons and two further 5′ exons designated C6 and C7. In our Y2H screen and in subsequent RT-PCR experiments (Fig. 3), we have found that human GPHN has at least four exons within the C4 cassette cluster; C4A, QIRRPDESKGVASRVGSLK (identical to original C4b cassette) (50); C4B, LHRKLEELRDHLEGNVKGYSLRVNVRFHL (novel exon); C4C, ARLPSCSSTYSVSE (identical to the original C4 cassette) (28); and C4D, LHSRLEGLKDELWRSRGYDLR (identical to the original C5 cassette) (25). The C4A-C-4B-C4C-C4D cluster is physically contiguous on human chromosome 14 BACS and definitively alters the genomic organization of *GPHN* (see Fig. 4).

The RT-PCR assays for human *GPHN* were designed to capture regions of splicing activity implicated from rodent *gphn* studies (Table I). Twelve different human RNA preparations from neurological (n = 4), and nonneurological (n = 8) tissues were tested (see Fig. 3*A*). The presence of rat *gphn* exons C1 (region 1) or exon C5* described by David-Watine (27) was not detected in any of our transcripts from human tissues. Exon C2 (region 1) was ubiquitously expressed in all transcripts with no suggestion of differential splicing. Furthermore, murine *gphn* exons C6 and C7 were not detected; nor was the exclusion of exon 18 in human *GPHN* transcripts (25, 51). The transcript pattern surrounding the C3 and C4 cluster revealed a clear difference between neurological tissues and nonneurological tissues. A solitary transcript was found in all nonneurological tissues, which included the C3 exon and excluded all exons from the C4 cluster (Fig. 3*A*). In contrast, neurological tissue generated a ladder effect, indicating the presence a range of fragments. The fragments were cloned into pGEM-easy vectors, and a total of 547 clones were PCR-screened for size differences, from which 86 clones were selected and sequenced. All of the clones sequenced contained perfectly preserved splicing insertion points and followed the linear 5′ to 3′ order of exons on the BAC contig. In total, sequencing confirmed the presence of 11 distinct neurological *GPHN* isoforms (Fig. 3*B*). The majority of neurological isoforms excluded exon C3 and contained a combination of the C4 exon cluster; however, two rare clones were detected that demonstrated the co-inclusion of exon C3 and one of the C4 cluster exons (Fig. 3*B*). One isoform corresponded to the nonneurological pattern by exclusively retaining the C3 exon, and this presumably reflects the metabolic transcript of gephyrin required in all tissues including the human brain.

To validate our capture of all transcript isoform combinations, further RT-PCRs were generated from an upstream invariant forward primer and nested reverse primers within each spliced exon of the C4 cluster (Table I). This approach captured all previously identified isoforms and did not reveal any additional isoform combinations. Finally, additional testing of the remaining *GPHN* invariant regions (Table I) found no evidence to suggest any exonic splicing outside the C3 and C4 exon cluster.

Mutation Analysis and SNP Distribution in GPHN—Three highly informative mutation detection techniques (SSCP, dideoxy fingerprinting, and automated dHPLC) were adopted to detect *GPHN* mutations and polymorphisms in a cohort of 32 hyperekplexia patients. Several SNPs were detected in the promoter, intronic, and exonic regions in both patient and control cohorts (Table II). In addition, a 4-bp deletion was detected within the *GPHN* candidate promoter region (del tgga at position $-976 \rightarrow -972$), which was also detected in normal controls and was not functionally assessed. Significantly, a heterozygous missense mutation (A28T) was detected in a hyperekplexia patient that causes an asparagine to tyrosine amino acid substitution (N10Y) in exon 1 of the *GPHN* gene (Fig. 5*A*). There were no restriction site changes for *GPHN* A28T, so consequently we analyzed 94 controls by DDF and confirmed the exclusion of patient-specific patterns from the control group (Fig. 5*B*). The N10Y substitution is positioned 5 amino acids upstream from a putative myristoylation site, which is a conserved marker for protein interactions with a membrane-bound receptor complex or the lipid bilayer of the plasma membrane. It was proposed that the N10Y mutation disturbed this interaction, thereby compromising the GPHN lattice at an anchorage point, leading to a disruption in GlyR

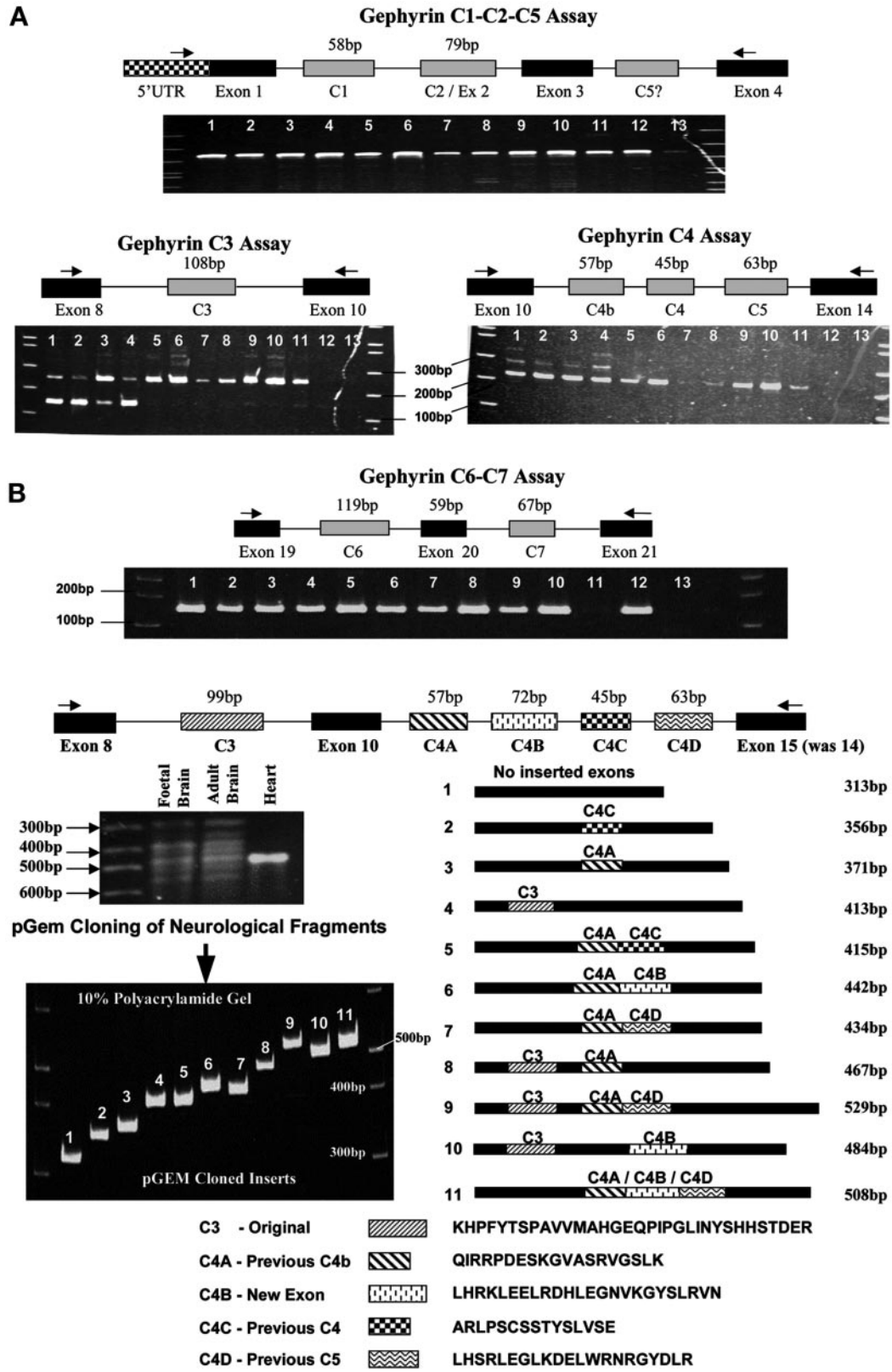

FIG. 3. **RT-PCR assays in putative regions of splicing activity in *GPHN*.** *A*, each of the four assays has primers anchored on invariant *GPHN*-P1 sequence (refer to Table I) and is based on prior knowledge of splicing activity (25, 28). Neurological tissues represent the first four samples in each gel (*left* to *right*: adult brain (*lane 1*); fetal brain (*lane 2*); spinal cord (*lane 3*); cerebellum (*lane 4*)), and samples 5–12 represent RT-PCR-derived nonneurological tissue (heart (*lane 5*); kidney (*lane 6*); pancreas (*lane 7*); lung (*lane 8*); liver (*lane 9*); fetal liver (*lane 10*); placenta (*lane 11*); and trachea (*lane 12*)), with *lane 13* representing a negative control PCR. Fragments were sized by a 1-kb ladder (Invitrogen). Only the C3 and C4 assays indicated the presence of transcript heterogeneity. *B*, size-ordered *GPHN*-pGEM clones derived from a C3/C4 cluster combination assay and digested with insert-releasing *Eco*RI restriction enzyme and resolved on a 10% polyacrylamide gel. In total, 11 neuronal *GPHN* isoforms were discovered, and each isoform corresponded to the expected sizes from the possible exonic combinations within the PCR assay. Each of the spliced exons are represented with distinct *patterns*, and amino acid translations are provided. Exons in the C4 cluster have been assigned a new nomenclature, and a conversion key relating to the old nomenclature is provided. Clone 4 was the sole transcript observed in nonneurological tissues ($n = 8$).

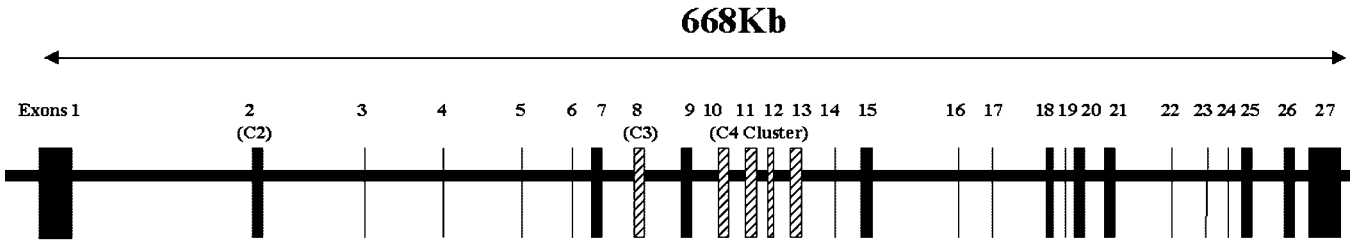

FIG. 4. **A revised genomic organization of human *GPHN*.** The previous version of the human *GPHN* gene described the existence of 27 exons distributed over 760 kb of genomic DNA on chromosome 14q32 (Fig. 2*A*). This remains true as a summary; however, our transcript data have led to a change in the order of exons, the exclusion of human exon C5*, and exclusion of rat C1, C6, and C7 from human *GPHN* transcripts. Based on these data, we suggest a new genomic representation of *GPHN* and a numbering system for all constitutional and spliced exons (Fig. 3*B*). We further recommend co-retaining the "C" nomenclatures for the C3 region and the (C4b-C4^{new}-C4-C5) cluster, with revision of the latter to the more logical labeling of C4A-C4B-C4C-C4D, reflecting the physical genomic organization of these exons within human *GPHN*.

TABLE I
RT-PCR primers for the spliced regions of GPHN

These primers were used in the generation and capture of human *GPHN* transcript isoforms. A *GPHN*-specific primer located at the 3′-end of the gene was used to generate cDNA fragments from mRNA templates derived from neurological (n = 4) and nonneurological (n = 8) tissues (Clontech). Primer sets for each candidate region of alternative splicing were designed in regions of the gene that were invariant from tissue to tissue. In addition, primer sets were designed to analyze the complete reading frame in order to exclude any further regions of exon splicing (Invariant 1 and 2). The exonic origin of each primer is shown in superscripts. Four nested primers located within each spliced exon were used in validation experiments to ensure capture of all *GPHN* transcript isoforms. UTR, untranslated region.

Assay	Forward primer 5′ → 3′	Reverse primer 5′ → 3′
Exonic 1st Strand Synthesis Primer	^{ex26}GTTCTTGGTGATGCCAAGTTAGTAT	
Region C1/2	$^{5'\text{-}UTR}$CTTCTCTGGCTCCCTAGCTGT	CCTGGCAGGTTAATTATGAGC^{ex6}
Region C3	^{ex7}CAGTGGTGTTGCTTCAACAGA	GCGATTCTGAAGGAGTAGTGC^{ex9}
Region C4/5	^{ex9}ACTCCATCATTTCTCGTGGTG	TCAGAGGAAAAGGAGACATGC^{ex14}
Region 6/7	^{ex17}ATCGTTTCATCATTGGGGAAT	ATTCCCTGTTGACATGACTGC^{ex20}
Combinatory C3-C4	^{ex7}CAGTGGTGTTGCTTCAACAGA	TCAGAGGAAAAGGAGACATGC^{ex14}
Invariant 1	^{ex14}AACATTCTCAGAGCCATCACA	CGGACAGCATAGCCATCTTTT^{ex18}
Invariant 2	^{ex20}ATCGCCATGACATTAAAAGAG	TGATCCTCGTCCAGAATACCA^{ex26}
Nested C3-C4A	^{ex7}CAGTGGTGTTGCTTCAACAGA	TTTGAGGGATCCAAC^{C4A}
Nested C3-C4B	^{ex7}CAGTGGTGTTGCTTCAACAGA	ATTTACTCTGAGAGA^{C4B}
Nested C3-C4C	^{ex7}CAGTGGTGTTGCTTCAACAGA	CTCAGATACACTATA^{C4C}
Nested C3-C4D	^{ex7}CAGTGGTGTTGCTTCAACAGA	TCTTAAGTCGTAGCC^{C4D}

TABLE II
Polymorphisms within GPHN

Sequence variations were initially discovered in the cohort of hyperekplexia patients. The approximate population frequency of each *GPHN* genotype was assessed in a variable number of unrelated Caucasian control samples using a variety of screening techniques as indicated by RFLP, DDF, or SSCP. UTR, untranslated region.

Sequence changes	Classification of change	Predicted consequence	Frequency in hyperekplexia	Frequency in controls	Assay
−972 del (tgga)	5′-UTR deletion	Unknown	1 from 31 (0.04)	1 from 58 (0.02)	SSCP
C-772T	SNP	Unknown	6 from 31 (0.20)	7 from 38 (0.18)	SSCP
A28T (ex 1)	Missense mutation	N10Y	1 from 31	0 from 94	DDF
IVS1 −9(T → C)	SNP	No effect	6 from 31 (0.20)	7 from 32 (0.22)	SSCP
IVS3 −38(G → A)	SNP	No effect	5 from 31 (0.16)	7 from 32 (0.22)	*Apo*I RFLP
IVS3 −6(T → C)	SNP	No effect	3 from 31 (0.10)	2 from 32 (0.07)	DDF
T1851C (ex 22)	SNP	No effect	1 from 31 (0.04)	1 from 48 (0.02)	*Aat*II RFLP
IVS24 −38(G → T)	SNP	No effect	1 from 31 (0.04)	2 from 32 (0.07)	*Hinc*II RFLP
IVS24 −14(A → T)	SNP	No effect	2 from 31 (0.07)	5 from 48 (0.10)	*Mbo*II RFLP
IVS25 −59(C → T)	SNP	No effect	3 from 31 (0.10)	5 from 48 (0.10)	SSCP

clustering and reduced attenuation of the startle response.

Functional Analysis of GPHN N10Y—To assess whether the mutation N10Y could affect interactions between GPHN with the GlyRs or with the GDP/GTP exchange factor collybistin, we carried out functional expression experiments in transfected human embryonic kidney cells (HEK293). We used expression constructs encoding (i) the GlyR β subunit intracellular loop tagged at the C terminus with red fluorescent protein (DSRed-GlyR β), (ii) collybistin II (CB2SH3-) tagged at the N terminus with the 9E10 (Myc) epitope, and (iii) gephyrin P1 wild-type and N10Y mutants tagged at the N terminus with EGFP. As expected, DSRed-GlyR β and Myc-CB2SH3 fusion proteins showed cytoplasmic expression (Fig. 6). In contrast, EGFP-gephyrin (not shown) and EGFP-gephyrin^{N10Y} formed small cytoplasmic aggregates that readily trap DSRed-GlyR β (Fig. 6). Since EGFP-gephyrin^{N10Y} is also translocated to the cell surface by collybistin II, it is unlikely that the N10Y mutation affects the structural lattice formed by gephyrin or interrupts gephyrin-GlyR β or gephyrin-collybistin interactions. These findings are reinforced by our yeast two-hybrid data, which strongly suggest that the GlyR β binding site on gephyrin is located within the C-terminal MoeA homology domain.

DISCUSSION

The pleiotropic nature of GPHN demands a molecular explanation, not only to account for the functional differences between neurological and nonneurological tissues but also to understand the basis for preferential recruitment and targeting of neurotransmitter receptors to the postsynaptic membrane. Derived from an extensive RT-PCR screen of the *GPHN*

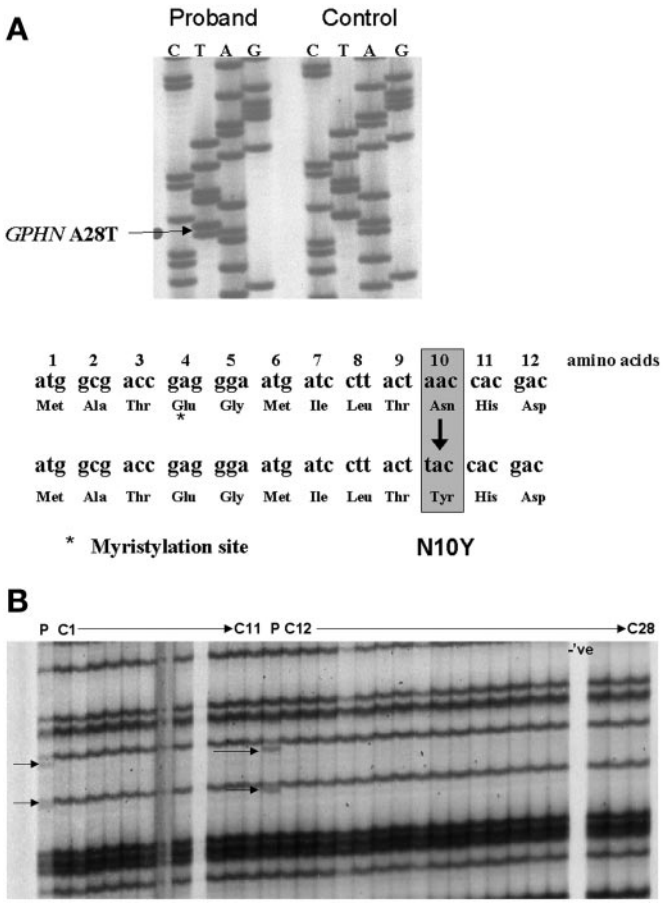

FIG. 5. **Mutation analysis of *GPHN* in hyperekplexia.** *A*, sequence analysis of *GPHN* exon 1 in a hyperekplexia patient using α-^{33}P cycle sequencing. A synonymous heterozygous change (A28T) was observed in exon 1 of *GPHN*, resulting in an N10Y amino acid substitution, positioned 6 residues upstream of a putative myristoylation site (28). *B*, a nondenaturing, 10% MDE gel illustrating a population study to compare patient *GPHN* A28T and population control DDF patterns. A patient-specific pattern (indicated by *arrows* in columns labeled *P*) was not detected in unrelated Caucasian control samples (n = 94; samples 1–28 illustrated).

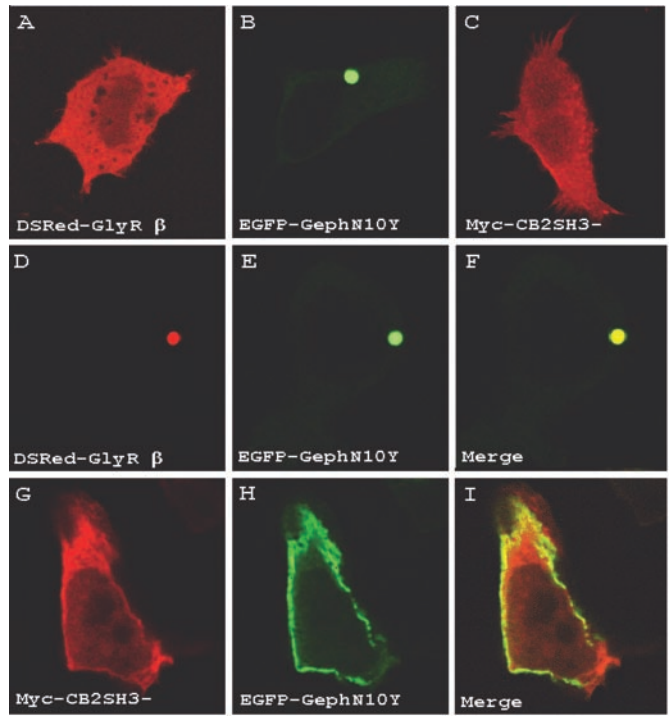

FIG. 6. **Functional assessment of GPHN-N10Y.** The expression assays demonstrate that the GPHN^{N10Y} mutation is unlikely to interfere with gephyrin-GlyR β subunit or gephyrin-collybistin interactions. When expressed alone in HEK293 cells, the GlyR β subunit intracellular loop tagged with red fluorescent protein (*A*; DSRed-GlyR β) and Myc-tagged collybistin II (*C*; Myc-CB2SH3-) are found throughout the cell. In contrast, note that EGFP-gephyrin^{N10Y} forms cytoplasmic aggregates (*B*), which are identical to those formed by EGFP-gephyrin. EGFP-gephyrin^{N10Y} readily traps DSRed-GlyR β in these cytoplasmic aggregates (*D–F*) and is translocated to the cell surface upon co-expression with collybistin II (*G–I*). The results reveal no significant differences compared with control experiments performed using nonmutated gephyrin (*i.e.* EGFP-gephyrin; data not shown).

gene and YTH clone capture, we provide evidence for extensive alternative intense splicing activity in neuronal tissue, which was in contrast to the single transcript observed in all eight nonneuronal tissues. The single nonneurological transcript includes exon C3, an exon that is absent from the majority of neuronal-specific transcripts, although human brain contains a mosaic expression of metabolic nonneuronal and heterogeneous neuron-specific isoforms. We suggest that the nonneuronal gephyrin transcript is ubiquitous in human tissues and serves a metabolic housekeeping purpose as a cofactor in molybdenum enzyme synthesis.

The substantial combinatory nature of the C4 exon cluster is created from four alternatively spliced exons, which generate 10 neuronal specific isoforms. The majority of these transcripts do not retain exon C3; however, two rarely detected isoforms have retained exon C3 and one of the C4 cluster exons. Three of the four exons observed in the C4 region have been reported in rodent tissues (25, 28). One novel exon was detected in human transcripts and is physically located, in the correct linear order, within the chromosome 14 BAC contig. Collectively, with the specific exon to exon construction pattern within all sequenced isoforms and the BAC contig validation, we are confident that the 5′ → 3′ order of the C3 and C4 spliced exons is correct. There remains a possibility that not all GPHN isoforms have been captured because of the sheer number of combinatory possibilities; however, any additional isoforms may be extremely rare and transcribed in specific areas of the human brain. In phylogenetic terms, our lack of detection for rodent exons C1, C6, and C7 in human tissue is also noted by David-Watine (27). It remains to be seen whether these exons exist, whether they are so weakly and specifically expressed that we did not detect them or whether they are an experimental artifact. For a gene that is so highly conserved, it is surprising that entire exons have been disregarded during recent evolution, but further work in rodents and human brain sections may be required to resolve this issue. It is significant, however, that rodent exons C6 and C7 are not detected, in a conserved or degenerate manner, within a small region of the chromosome 14 BAC contig containing the expected insertion points between exons 15 and 19 of *GPHN*. All remaining 27 human *GPHN* exons (including C3 and C4 cluster) are easily detectable on the BAC contig by BLAST comparison with homologous rodent exons. In summary, the YTH and PCR results demonstrate that (i) the complexity of alternative splicing of gephyrin has been greatly underestimated; (ii) a revised genomic structure for human *GPHN* and a simplified nomenclature for the exons within the C4 cluster is required; (iii) the GlyR β subunit is capable of interacting with multiple gephyrin isoforms; and (iv) molecular mechanisms exist whereby gephyrin could regulate complex associations with different cytoskeletal or cytoplasmic proteins at glycinergic *versus* GABAergic synapses.

The speculative functional consequence of the heterogeneous GPHN isoforms is attributed to interactions with a complex repertoire of protein interactions. The present list includes

evidence for protein interactions with the β subunit of the glycine receptor, tubulin, GABARAP, profilin, collybistin, and the dynein light chains. Considering that this is probably not the complete cast of interacting proteins, it becomes apparent that the splicing activity of C3 and C4 regions of the *GPHN* gene may form the basis for differential properties of GPHN isoforms. The "linker" segment also contains several potential protein-protein interaction domains including proline-rich and acidic segments as well as a short motif (amino acids 289–299) that has strong similarity to the tubulin-binding domain signature of tau and MAP2/MAP4 proteins (25). This may be of significance, since the tubulin-binding properties of gephyrin closely resemble those of mitogen-activated proteins (52). Given the proximity of the site of insertion for the C4 cassette to the putative tubulin-binding domain, it is possible that C4 inserts might influence interactions with cytoskeletal proteins.

Interestingly, cassettes C4B and C4D are homologous to each other and to the α-helical region 1B of human keratin 8 (53). This motif is known to mediate keratin dimerization by the formation of coiled-coil structures. It is possible that inclusion of cassettes C4B and or C4D creates a binding site for a new gephyrin interactor. Ramming *et al.* (25) concluded that gephyrin transcripts containing the C3 and C4 exons were of low abundance but highly expressed in some subpopulations of neurons in the adult mouse brain. For example, cassette C4D was found in the granular cell layer of the cerebellum and olfactory bulb. However, this study did not take other developmental stages into account (*e.g.* cassette C3 is highly expressed throughout the central nervous system early in development) and did not focus on spinal cord or brainstem. Generating spliced exon-specific antibodies and immunohistochemical analysis in rodent and human brain will greatly enhance our understanding of spatial and temporal distribution of gephyrin transcripts.

Despite the established association of hyperekplexia mutations with subunits from glycinergic ion channels in both humans and animal models, it is apparent that mutations in gephyrin are not a major cause of the disorder. Considering the high degree of phylogenetic conservation and that GPHN is an essential metabolic agent, it is possible that mutations in many regions of *GPHN* are embryonic lethal. Our promoter and exon by the exon mutation detection approach revealed a novel mutation causing a N10Y substitution at the extreme N terminus of GPHN. This portion of gephyrin is not part of the MogA consensus sequence, which begins at amino acid 15, and this positioning may be the basis of functional tolerance in the mutation carrier. Recent crystal structure determination of the GPHN N-terminal domain indicates a trimeric structure that presumably is the structural conformation required to form a subsynaptic lattice (54, 55). The N10Y mutation was found in a young male infant who presented with neonatal hypertonia and excessive startle response in the first year of life. At 4 years of age, there has been a transient recovery of the phenotype with no features of molybdenum metabolism disruption. $GPHN^{N10Y}$ may have a limited detrimental window during developmental glycinergic switching from GlyR α_2 homopentamers to GlyR $\alpha_{1\beta}$ heteropentamers. From a glycinergic perspective, $GPHN^{N10Y}$ does not disrupt GlyR-gephyrin interactions in human embryonic kidney cells and does not interrupt collybistin-induced cell surface clustering. Since *in vitro* clustering is not affected by $GPHN^{N10Y}$, the functional effect of this mutation remains elusive, and an alternative mechanism is responsible for the hyperekplexia phenotype.

The fact remains, however, that ~60% of our sporadic hyperekplexia cohort is devoid of *GLRA1*, *GLRB*, and *GPHN* mutations, and this clearly implies further genetic heterogeneity. Casting a wider net for the mutation analysis of glycinergic transporters and GABAergic candidates may yet yield further genetic heterogeneity in hyperekplexia. Indeed, recent descriptions of $GABA_A$ mutations in epilepsy demonstrates the subtle functional overlap between the two neuroinhibitory systems with the resulting phenotypes a reflection of the differential localizations and function of glycinergic and GABAergic receptor subunit expression.

In conclusion, we have demonstrated the existence of a large number of neuron-specific gephyrin isoforms that may form the basis for specialized protein interactions. By identifying all exon constituents of the gene, we were able to exclude the gephyrin coding sequence as a major determinant for hyperekplexia. Nevertheless, a solitary mutation may yet have a functional explanation in a transient form of the disorder despite the exclusion of our initial functional hypothesis. We describe a number of synonymous and flanking intronic SNPs of *GPHN* that may be informative for mapping purposes and other disorders linked to chromosome 14q24. Finally, as a consequence of a YTH search for glycinergic interacting proteins, we can confirm that the physical location of the GPHN-GlyR β interacting domain in the GPHN molecule does not lie in the MogA region, linker segment, or C3 and C4 splicing cluster. This domain lies within the C-terminal portion of the conserved MoeA region, and the definitive identification of an interacting GPHN motif represents the next challenge toward characterizing the physical nature of GPHN-GlyR coupling.

Acknowledgments—We thank Helena de Silva for HEK293 cell culture and transfections and Professor Alan Hall (University College London) for providing the pRK5myc plasmid.

REFERENCES

1. Grenningloh, G., Rienitz, A., Schmitt, B., Methfessel, C., Zensen, M., Beyreuther, K., Gundelfinger, E. D., and Betz, H. (1987) *Nature* **328,** 215–220
2. Langosch, D., Becker, C. M., and Betz, H. (1990) *Eur. J. Biochem.* **194,** 1–8
3. Langosch, D., Thomas, L., and Betz, H. (1988) *Proc. Natl. Acad. Sci. U. S. A.* **85,** 7394–7398
4. Betz, H. (1991) *Trends Neurosci.* **14,** 458–461
5. Kuhse, J., Laube, B., Magalei, D., and Betz, H. (1993) *Neuron* **11,** 1049–1056
6. Langosch, D., Hoch, W., and Betz, H. (1992) *FEBS Lett.* **298,** 113–117
7. Meyer, G., Kirsch, J., Betz, H., and Langosch, D. (1995) *Neuron* **15,** 563–572
8. Kneussel, M., Hermann, A., Kirsch, J., and Betz, H. (1999) *J. Neurochem.* **72,** 1323–1326
9. Kannenberg, K., Baur, R., and Sigel, E. (1997) *J. Neurochem.* **68,** 1352–1360
10. Essrich, C., Lorez, M., Benson, J. A., Fritschy, J. M., and Luscher, B. (1998) *Nat. Neurosci.* **1,** 563–571
11. Baer, K., Essrich, C., Benson, J. A., Benke, D., Bluethmann, H., Fritschy, J. M., and Luscher, B. (1999) *Proc. Natl. Acad. Sci. U. S. A.* **96,** 12860–12865
12. Kneussel, M., Brandstatter, J. H., Laube, B., Stahl, S., Muller, U., and Betz, H. (1999) *J. Neurosci.* **19,** 9289–9297
13. Sassoe-Pognetto, M., Panzanelli, P., Sieghart, W., and Fritschy, J. M. (2000) *J. Comp. Neurol.* **420,** 481–498
14. Kneussel, M., and Betz, H. (2000) *J. Physiol.* **525,** 1–9
15. Pfeiffer, F., Graham, D., and Betz, H. (1982) *J. Biol. Chem.* **257,** 9389–9393
16. Graham, D., Pfeiffer, F., Simler, R., and Betz, H. (1985) *Biochemistry* **24,** 990–994
17. Kirsch, J., Langosch, D., Prior, P., Littauer, U. Z., Schmitt, B., and Betz, H. (1991) *J. Biol. Chem.* **266,** 22242–22245
18. Meier, J., Vannier, C., Serge, A., Triller, A., and Choquet, D. (2001) *Nat. Neurosci.* **4,** 253–260
19. Kirsch, J., Wolters, I., Triller, A., and Betz, H. (1993) *Nature* **366,** 745–748
20. Feng, G., Tintrup, H., Kirsch, J., Nichol, M. C., Kuhse, J., Betz, H., and Sanes, J. R. (1998) *Science* **282,** 1321–1324
21. Sabatini, D. M., Barrow, R. K., Blackshaw, S., Burnett, P. E., Lai, M. M., Field, M. E., Bahr, B. A., Kirsch, J., Betz, H., and Snyder, S. H. (1999) *Science* **284,** 1161–1164
22. Mammoto, A., Sasaki, T., Asakura, T., Hotta, I., Imamura, H., Takahashi, K., Matsuura, Y., Shirao, T., and Takai, Y. (1998) *Biochem. Biophys. Res. Commun.* **243,** 86–89
23. Kins, S., Betz, H., and Kirsch, J. (2000) *Nat. Neurosci.* **3,** 22–29
24. Fuhrmann, J. C., Kins, S., Rostaing, P., El Far, O., Kirsch, J., Sheng, M., Triller, A., Betz, H., and Kneussel, M. (2002) *J. Neurosci.* **22,** 5393–5402
25. Ramming, M., Kins, S., Werner, N., Hermann, A., Betz, H., and Kirsch, J. (2000) *Proc. Natl. Acad. Sci. U. S. A.* **97,** 10266–10271
26. Rees, M. I. (2001) *Am. Soc. Hum. Genet.* **69,** 627 (Abstr. 2623)
27. David-Watine, B. (2001) *Gene (Amst.)* **271,** 239–245
28. Prior, P., Schmitt, B., Grenningloh, G., Pribilla, I., Multhaup, G., Beyreuther, K., Maulet, Y., Werner, P., Langosch, D., Kirsch, J., and Betz, H. (1992) *Neuron* **8,** 1161–1170

29. Sassoe-Pognetto, M., Kirsch, J., Grunert, U., Greferath, U., Fritschy, J. M., Mohler, H., Betz, H., and Wassle, H. (1995) *J. Comp. Neurol.* **357,** 1–14
30. Kawasaki, B. T., Hoffman, K. B., Yamamoto, R. S., and Bahr, B. A. (1997) *J. Neurosci. Res.* **49,** 381–388
31. Stallmeyer, B., Schwarz, G., Schulze, J., Nerlich, A., Reiss, J., Kirsch, J., and Mendel, R. R. (1999) *Proc. Natl. Acad. Sci. U. S. A.* **96,** 1333–1338
32. Kirsch, J. (1999) *Curr. Opin. Neurobiol.* **9,** 329–335
33. Kirsch, J., Malosio, M. L., Wolters, I., and Betz, H. (1993) *Eur. J. Neurosci.* **5,** 1109–1117
34. Shiang, R., Ryan, S. G., Zhu, Y. Z., Hahn, A. F., O'Connell, P., and Wasmuth, J. J. (1993) *Nat. Genet.* **5,** 351–358
35. Rees, M. I., Andrew, M., Jawad, S., and Owen, M. J. (1994) *Hum. Mol. Genet.* **3,** 2175–2179
36. Rees, M. I., Lewis, T. M., Vafa, B., Ferrie, C., Corry, P., Muntoni, F., Jungbluth, H., Stephenson, J. B., Kerr, M., Snell, R. G., Schofield, P. R., and Owen, M. J. (2001) *Hum. Genet.* **109,** 267–270
37. Rees, M. I., Lewis, T. M., Kwok, J. B., Mortier, G. R., Govaert, P., Snell, R. G., Schofield, P. R., and Owen, M. J. (2002) *Hum. Mol. Genet.* **11,** 853–860
38. Andermann, F., Keene, D. L., Andermann, E., and Quesney, L. F. (1980) *Brain* **103,** 985–997
39. Saenz-Lope, E., Herranz-Tanarro, F. J., Masdeu, J. C., and Chacon Pena, J. R. (1984) *Ann. Neurol.* **15,** 36–41
40. Brown, P. (2002) *Adv. Neurol.* **89,** 153–159
41. Butler, M. H., Hayashi, A., Ohkoshi, N., Villmann, C., Becker, C. M., Feng, G., De Camilli, P., and Solimena, M. (2000) *Neuron* **26,** 307–312
42. Reiss, J., Gross-Hardt, S., Christensen, E., Schmidt, P., Mendel, R. R., and Schwarz, G. (2001) *Am. J. Hum. Genet.* **68,** 208–213
43. Handford, C. A., Lynch, J. W., Baker, E., Webb, G. C., Ford, J. H., Sutherland, G. R., and Schofield, P. R. (1996) *Brain Res. Mol. Brain Res.* **35,** 211–219
44. Fuller, K. J., Morse, M. A., White, J. H., Dowell, S. J., and Sims, M. J. (1998) *BioTechniques* **25,** 85–88, 90–92
45. Harvey, R. J., Vreugdenhil, E., Zaman, S. H., Bhandal, N. S., Usherwood, P. N., Barnard, E. A., and Darlison, M. G. (1991) *EMBO J.* **10,** 3239–3245
46. Dunne, E. L., Hosie, A. M., Wooltorton, J. R., Duguid, I. C., Harvey, K., Moss, S. J., Harvey, R. J., and Smart, T. G. (2002) *Br. J. Pharmacol.* **137,** 29–38
47. Budowle, B., Chakraborty, R., Giusti, A. M., Eisenberg, A. J., and Allen, R. C. (1991) *Am. J. Hum. Genet.* **48,** 137–144
48. Sarkar, G., Yoon, H. S., and Sommer, S. S. (1992) *Genomics* **13,** 441–443
49. Liu, Q., Feng, J., and Sommer, S. S. (1996) *Hum. Mol. Genet.* **5,** 107–114
50. Heck, S., Enz, R., Richter-Landsberg, C., and Blohm, D. H. (1997) *Brain Res. Dev. Brain Res.* **98,** 211–220
51. Meier, J., De Chaldee, M., Triller, A., and Vannier, C. (2000) *Mol. Cell Neurosci.* **16,** 566–577
52. Kirsch, J., Meyer, G., and Betz, H. (1996) *Mol. Cell Neurosci.* **8,** 93–98
53. Krauss, S., and Franke, W. W. (1990) *Gene* (*Amst.*) **86,** 241–249
54. Schwarz, G., Schrader, N., Mendel, R. R., Hecht, H. J., and Schindelin, H. (2001) *J. Mol. Biol.* **312,** 405–418
55. Sola, M., Kneussel, M., Heck, I. S., Betz, H., and Weissenhorn, W. (2001) *J. Biol. Chem.* **276,** 25294–25301